Relaxation Filtered Hyperfine (REFINE) Spectroscopy: A Novel Tool for Studying Overlapping Biological Electron Paramagnetic Resonance Signals Applied to Mitochondrial Complex I†

Thorsten Maly,‡ Fraser MacMillan,‡ Klaus Zwicker,§ Noushin Kashani-Poor,§ Ulrich Brandt,§ and Thomas F. Prisner*,‡

Institut für Physikalische und Theoretische Chemie and Zentrum für Biomolekulare Magnetische Resonanz, Johann Wolfgang Goethe-Universität Frankfurt, D-60439 Frankfurt am Main, Germany, and Institut für Biochemie I, Zentrum der Biologischen Chemie, Universitätsklinikum Frankfurt, D-60590 Frankfurt am Main, Germany

Received October 16, 2003; Revised Manuscript Received January 30, 2004

ABSTRACT: A simple strategy to separate overlapping electron paramagnetic resonance (EPR) signals in biological systems is presented. Pulsed EPR methods (inversion- and saturation-recovery) allow the determination of the T_1 spin-lattice relaxation times of paramagnetic centers. T_1 may vary by several orders of magnitude depending on the species under investigation. These variations can be employed to study selectively individual species from a spectrum that results from an overlap of two species using an inversion-recovery filtered (IRf) pulsed EPR technique. The feasibility of such an IRf field-swept technique is demonstrated on model compounds (α,γ-bisphenylene-β-phenylallyl-benzolate, BDPA, and 2,2,6,6-tetramethyl-piperidine-1-oxyl, TEMPO) and a simple strategy for the successful analysis of such mixtures is presented. Complex I is a multisubunit membrane protein of the respiratory chain containing several iron-sulfur (FeS) centers, which are observable with EPR spectroscopy. It is not possible to investigate the functionally important FeS cluster N2 separately because this EPR signal always overlaps with the other FeS signals. This cluster can be studied selectively using the IRf field-swept technique and its EPR spectrum is in excellent agreement with previous cw-EPR data from the literature. In addition, the possibility to separate the hyperfine spectra of two spectrally overlapping paramagnetic species is demonstrated by applying this relaxation filter together with hyperfine spectroscopy (REFINE). For the first time, the application of this filter to a three-pulse electron spin-echo envelope modulation (ESEEM) pulse sequence is demonstrated to selectively observe hyperfine spectra on a system containing two paramagnetic species. Finally, REFINE is used to assign the observed nitrogen modulation in complex I to an individual iron-sulfur cluster.

Paramagnetic iron-sulfur (FeS) clusters are commonly observed in the electron paramagnetic resonance (EPR)[1] spectra of many biological systems. They play an important role in the translocation of electrons in enzymes (*1*). Their detection and classification can be performed with continuous wave (cw)-EPR; however, a common problem is the presence of more than one species, and the separation of their EPR signals is crucial to characterize them in more detail using, for example, hyperfine spectroscopy. Several membrane proteins in which FeS clusters are found have already been crystallized and their structures determined (*2*). The NADH: ubiquinone oxidoreductase (complex I) from the mitochondrial respiratory chain is among the largest and most complex membrane-bound multiprotein complexes known (*3*, *4*), but currently little structural information is available. Complex I is the first complex of the mitochondrial respiratory chain and links the electron transfer from NADH to ubiquinone with the concomitant translocation of four protons across the inner membrane (*5*, *6*). Despite its central role in eukaryotic oxidative phosphorylation and its involvement in a broad range of human disorders (*7*), little is known about its structure and catalytic mechanism. Cw-EPR experiments have demonstrated the presence of several FeS clusters in complex I (*8*−*10*), although the characterization of the individual paramagnetic centers is rather difficult due to their similar spectroscopic properties. In general, complex I contains one molecule of noncovalently bound flavine mononucleotide and, depending on the organism, as many as eight iron-sulfur (FeS) clusters (2 × [2Fe−2S] and

† This work was supported by the Sonderforschungsbereich SFB 472 "Molecular Bioenergetics", Projects P2 and P15, the Hermann Willkomm Stiftung (to T.M. and F.M.), the Zentrum für Biomolekulare Magnetische Resonanz, and Fonds der Chemischen Industrie.

* Corresponding author: Fax (+49) 69 798 29406, phone (+49) 69 798 29404, e-mail prisner@chemie.uni-frankfurt.de.

‡ Johann Wolfgang Goethe-Universität Frankfurt.

§ Universitätsklinikum Frankfurt.

[1] Complex I, NADH:ubiquinone oxidoreductase; CuHis, copper-doped *l*-histidine model complex; BDPA, α,γ-bisphenylene-β-phenylallyl-benzolate; cw, continuous wave; ESEEM, electron spin-echo envelope modulation; ENDOR, electron nuclear double resonance; EPR, electron paramagnetic resonance; FeS, iron-sulfur; HYSCORE, hyperfine sublevel correlation; IRf, inversion-recovery filtered; NADH, nicotinamide adenine dinucleotide; PELDOR, pulsed electron electron double resonance; REFINE spectroscopy, relaxation filtered hyperfine spectroscopy; S/N, signal-to-noise; TEMPO, 2,2,6,6-tetramethyl-piperidine-1-oxyl; T_F, filter time; TRIPLE, electron nuclear nuclear triple resonance; G, Gauss.

10.1021/bi035865e CCC: $27.50
Published on Web 03/05/2004

6 × [4Fe−4S]) as electron-transfer components (*8*), although to date only six FeS clusters have been observed using EPR spectroscopy. According to the assignment of complex I from bovine heart mitochondria, they are designated N1a and N1b for the [2Fe−2S] clusters and N2, N3, N4, and N5 for [4Fe−4S] clusters, which is based upon their temperature-dependent appearance in the cw-EPR spectrum (*8*). Because of its comparatively high pH-dependent redox potential (*11*) and its putative interaction with a semiquinone radical (*12*), cluster N2 has been proposed to play a prominent role in redox-linked proton translocation (*13*, *14*). It has been shown that cluster N2 is located on the PSST subunit of complex I (*15*, *16*), but in this subunit only three cysteines are available to form the usual binding motif for a tetranuclear iron-sulfur cluster. This raised the question about the nature and the location of the fourth ligand of cluster N2. The obligate aerobic yeast *Yarrowia lipolytica* represents a powerful model system to study complex I (*17*). By a combination of site-directed mutagenesis, enzyme kinetics, and EPR spectroscopy, it was possible to obtain new insights into the nature of the catalytic core of complex I (*18*, *19*). As a result of these studies, the nitrogen-containing amino acids arginine-141 and histidine-226 in the 49 kDa subunit were suggested as candidates to ligate iron-sulfur cluster N2. The interaction of nitrogen-containing amino acids with iron-sulfur centers can be studied using electron spin-echo envelope modulation (ESEEM) spectroscopy (*20*−*22*). In cw-EPR at low temperatures (<25 K), the N2 spectrum is strongly overlapped with the spectrum of cluster N1. So far N1 is the only binuclear cluster detected in complex I from *Y. lipolytica*. N1 becomes reduced by NADH, and because of its EPR-spectroscopic properties, it is assumed that this cluster corresponds to cluster N1b in the bovine enzyme. N1b is located in the 75 kDa subunit, which possesses three conserved cysteine binding motifs for iron-sulfur clusters (*8*).

The spectral overlap of paramagnetic species is a common problem in the EPR investigation of biological systems but in many cases different paramagnetic species can, in principle, be distinguished by one of their EPR parameters. If the paramagnetic species have different *g*-values, they can be separated by performing high-field, high-frequency EPR spectroscopy (*23*) because the **g**-tensor is field-dependent. Thus just as in nuclear magnetic resonance (NMR) spectroscopy, higher magnetic fields lead to a higher resolution of the EPR spectrum. An alternative method to separate overlapping species by their **g**-tensor values at X-band frequencies (9−10 GHz) is electron-Zeeman-resolved EPR, a method whereby a variable-amplitude, external sinusoidal modulated field is applied, resulting in a field-swept EPR spectrum that is spread into a second dimension, representing the *g*-values of the paramagnetic species (*24*).

If the overlapping species have different electronic spin quantum numbers S and m_s, they can be distinguished by their different Rabi-oscillation (nutation) frequencies. The phase-inverted echo-amplitude-detected nutation (PEANUT) experiment allows the separation of paramagnetic species according to their different nutation frequencies (*25*). A two-dimensional PEANUT experiment, which correlates such nutation frequencies to the resonant field, simplifies the interpretation of such complex field-swept EPR spectra. Another possibility to separate paramagnetic species with different spin quantum numbers S or m_s is by their refocusing time, which is also a function of S and m_s (*26*).

With time-domain techniques that exploit the spin-lattice relaxation time (T_{1e}) and their temperature dependency, it is also possible to distinguish between different species. With the filter effect of the stimulated echo sequence with respect to the longitudinal relaxation time, it is possible to suppress the contribution of one species (*27*, *28*). Longitudinal detection can also be used to separate EPR signals by their differences in T_{1e} (*29*).

Here we describe a general concept to filter-pulsed EPR spectra based upon T_1 relaxation differences. An inversion-recovery filter (IRf) applied together with pulsed EPR allows the separation of paramagnetic species by their differences in the longitudinal relaxation time, T_{1e}, and other processes contributing to the recovery of the magnetization. Depending on the filter time (T_F) chosen, it is possible to selectively suppress one of the overlapping species and thus in the case of two species record an EPR spectrum of the second species. The inversion-recovery filter can in principle be combined with many pulse experiments, such as echo-detected field-swept EPR, ESEEM, HYSCORE, ENDOR, or PELDOR. Here we introduce the principle of relaxation-filtered hyperfine (REFINE) spectroscopy by applying this filter together with a three-pulse ESEEM sequence (*30*) on a mixture of BDPA and CuHis to demonstrate that it is possible with this method to record separated hyperfine spectra. The REFINE method is then applied to mitochondrial complex I to assign the nitrogen modulations observed in the ESEEM spectrum of the iron-sulfur clusters N1 and N2. The requirements in a mixture of two paramagnetic species with respect to cw-signal-to-noise (S/N) ratio, intensity, and longitudinal relaxation time ratio are discussed.

MATERIALS AND METHODS

The well-known organic radicals TEMPO (2,2,6,6-tetramethyl-piperidine-1-oxyl) and BDPA (α,γ-bisphenylene-β-phenylallyl-benzolate) are employed as model systems to demonstrate the efficiency of the REFINE method. All model compounds and their mixtures are first dissolved in a solution of polystyrene in toluene. The solutions are then evaporated (293 K) and finally dried in high vacuum (10^{-5} mbar) to ensure that all solvent molecules are removed. The final concentration for all samples is about 5×10^{-6} mol/kg. For the IRf field-swept experiments, the weight ratio of TEMPO/BDPA is chosen such that the maximum intensity of the BDPA EPR line in absorption is of the same order of the intensity of the central line of the TEMPO spectrum. Copper-doped histidine (CuHis) is prepared from a deuterated aqueous (D_2O) solution of *l*-histidine hydrochloride containing 0.5% (mole) anhydrous copper sulfate ($CuSO_4$) by slow evaporation. A CuHis/BDPA ratio of 26/1 (w/w) results in a 1/9 intensity ratio at the magnetic field position of the BDPA EPR resonance.

The yeast *Y. lipolytica* is a powerful model system for structural and functional analysis of complex I. It combines the availability of a preparation procedure resulting in a pure, stable, and enzymatically active enzyme complex together with the opportunity to use site-directed mutagenesis for functional and structural analysis (*17*, *31*). Growth of *Y. lipolytica* and preparation of isolated complex I is performed as described (*32*).

EPR samples are prepared using isolated complex I mixed with the physiological substrate nicotinamide adenine dinucleotide (NADH) directly in the EPR tube and frozen in liquid nitrogen after 30 s reaction time. The cw-EPR spectrum from complex I reduced with NADH reveals signals originating from five different FeS clusters: N1 (2Fe−2S), N2, N3, N4, and N5 (all 4Fe−4S) (*33*).

X-Band spectra are measured on a Bruker E-580 spectrometer using a Bruker EPR cavity (MD5-W1) equipped with an Oxford helium flow cryostat (CF935). The pulses are amplified using a 1 kW pulsed travelling wave tube (TWT) amplifier for complex I and CuHis/BDPA or a 20 W cw-TWT for the TEMPO/BDPA mixture. Conventional ($\pi/2-\tau-\pi$) and IRf ($\pi-T_F-\pi/2-\tau-\pi$) field-swept spectra are obtained by integrating the area under a Hahn echo as a function of the magnetic field. For inversion-recovery time traces at fixed field positions, all traces are normalized to the echo amplitude without an inversion pulse. For REFINE, a three-pulse stimulated echo sequence is combined with the inversion-recovery filter resulting in a four-pulse sequence ($\pi-T_F-\pi/2-\tau-\pi/2-T-\pi/2$). To remove all unwanted echoes, a full eight-step phase cycle is applied for the IRf field-swept sequence, while a 16-step phase cycle (*34*) is used for REFINE.

For quantitative analysis and comparison, the S/N ratio is given for a time constant of 1 s in cw-EPR and 1 s averaging time for pulsed experiments.

The ideal pulse length using the 20 W TWT for the TEMPO/BDPA mixture is 96 ns for the π inversion and the π pulse and 48 ns for the $\pi/2$ pulse. The pulse lengths used for the IRf-field-swept experiment on complex I are set to 16 ns for the π pulse and 8 ns for the $\pi/2$ pulse. For REFINE on the model system, the pulse lengths are optimized to 20 ns for the inversion π pulse and 12 ns for the $\pi/2$ pulse. REFINE spectra are recorded at a fixed value of T_F while incrementing the time T in steps of 16 ns. Five hundred twelve points are taken in the time domain. For all ESEEM spectra, a τ value of 172 ns is used.

For the biological system complex I, the pulse lengths are set to 12 ns for the inversion π pulse and 24 ns for the $\pi/2$ pulse. REFINE spectra are recorded at a fixed value of T_F while incrementing the time T in steps of 20 ns. Two hundred fifty-six points are taken in the time domain at a τ value of 192 ns.

Data fitting is performed using a least-squares fit routine in Origin. For REFINE spectra, a second-order polynomial background (model complexes) or a low-pass (ν_{cutoff} = 0.5 MHz) filtered time trace (complex I) is subtracted from the time traces to remove the echo decay function. Before Fourier transformation, a Hanning window function is applied and the time trace is zero-filled to double the number of experimental data points. Magnitude Fourier spectra are shown in all cases. Due to a spurious baseline artifact, the first 20 data points in the time traces of complex I are ignored. Field-swept echo-detected EPR spectra of N1 and N2 are numerically simulated using a powder average of 4144 molecules equally distributed on a unit sphere with respect to their orientation relative to the external magnetic field vector $\mathbf{B}_0$. The resulting histogram is convoluted with a Gaussian line to account for the inhomogeneous line width of unresolved hyperfine interactions. All measurements are compared to a *g*-standard (BDPA in polystyrene) to accurately adjust the field position.

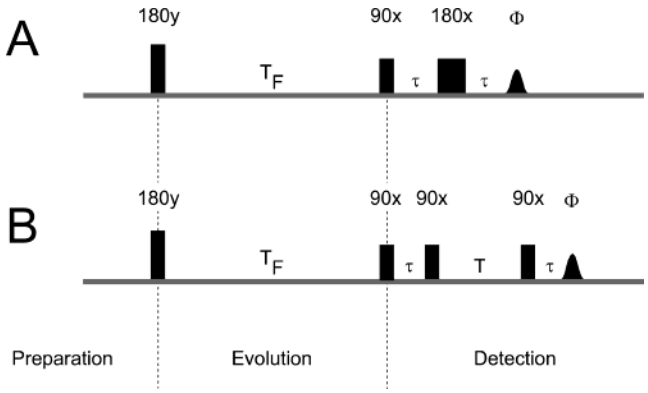

FIGURE 1: Pulse sequences. To vary the amplitudes independently, the pulses were set in two different microwave channels as indicated by the corresponding indices. Panel A depicts the IRf field-swept sequence. An eight-step phase cycling is required to remove the contribution of unwanted echoes. Panel B depicts the REFINE sequence using a three-pulse ESEEM sequence. A 16-step phase cycling is required to remove the contribution of all unwanted echoes.

RESULTS

1. Model Compounds. The pulse sequences used to perform inversion-recovery filtered experiments are shown in Figure 1. As is commonly used in NMR, the sequences are distinguished into three different time segments: preparation (P), evolution (E), and detection (D). During the preparation (P), a non-Boltzmann polarization, $-M_Z$, of the electron spin magnetization is created by a π (180°) inversion pulse. Due to longitudinal relaxation, the electron spin will relax back to the thermal equilibrium magnetization, M_Z^∞, during the evolution (E) time period. This relaxation back to the thermal equilibrium polarization can be monitored by using a Hahn echo (Figure 1A) or a stimulated echo (Figure 1B) detection sequence (D) by varying the time T_F between preparation and detection. This is typically done in an inversion-recovery experiment from which it is in principle possible to obtain the transversal relaxation time, T_1.

It is a well-known problem that relaxation times measured by the inversion-recovery method are often described by nonexponential decays. This is because quite often it is not possible to completely invert the entire spectrum using a single microwave pulse. In this case, other processes such as spectral diffusion may also contribute to the observed magnetization recovery (*35*) and often result in an overall nonexponential decay. In the simplest case, the inversion-recovery time trace of such a system can be described by a two-exponential function

$$\Phi(t) = 1 - I^f \exp\left(\frac{-t}{T^f}\right) - I^s \exp\left(\frac{-t}{T^s}\right) \qquad (1)$$

where I and T are the amplitudes and time constants, respectively, for a slow (s) and fast (f) component where the slow component is close to the true value of T_{1e}. No further attempts are made to analyze the decay function in more detail, because it is not important to know exactly the origin of the different processes contributing to the whole relaxation decay for the filter method presented here.

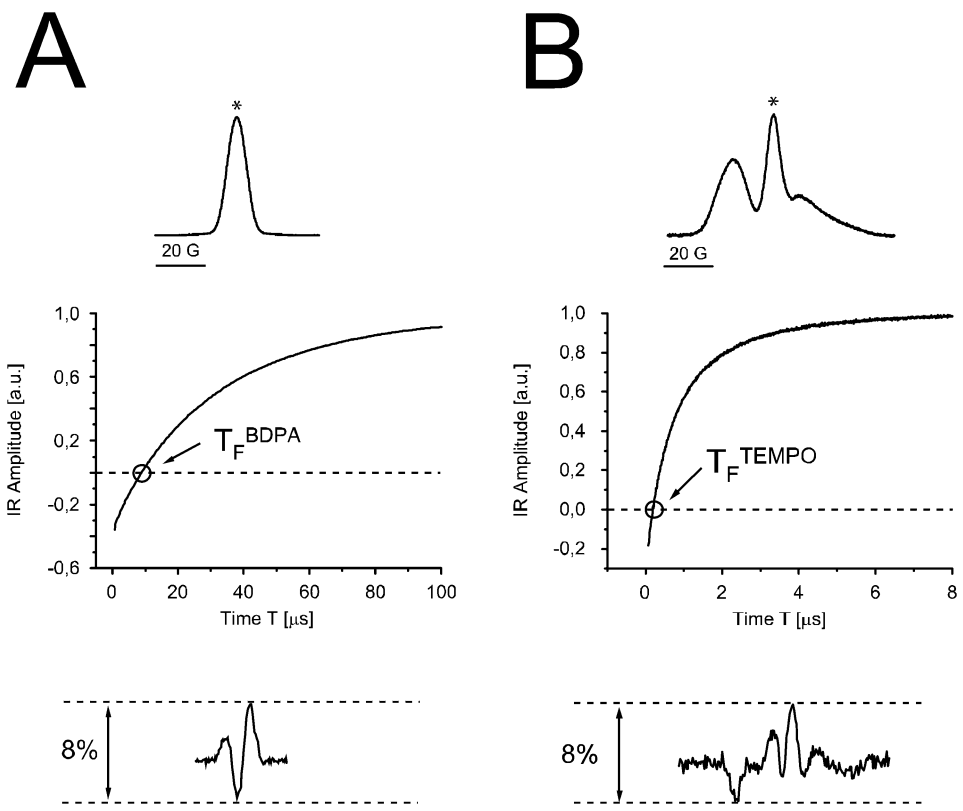

FIGURE 2: Inversion-recovery traces of the individual model compounds. All inversion-recovery traces and field-swept spectra are recorded at room temperature. Field positions for inversion-recovery traces are marked in the EPR spectra by asterisks. Fit parameters for inversion-recovery traces are given in Table 1. Panel A depicts (top) the field-swept spectrum of BDPA, (middle) the inversion-recovery trace of BDPA in polystyrene, and (bottom) the IRf field-swept spectrum of BDPA at $T_F = 9$ μs. Panel B depicts (top) the field-swept spectrum of TEMPO, (middle) the inversion-recovery trace of TEMPO in polystyrene, and (bottom) the IRf field-swept spectrum of TEMPO at $T_F = 192$ ns.

In Figure 2A,B, the inversion-recovery traces and the respective EPR spectra for the two pure compounds, BDPA and TEMPO, are shown. The magnetic field positions for the inversion-recovery measurements are marked with an asterisk in the field-swept spectra at the top of the respective representation. After inversion of the electron spin magnetization, this magnetization decay traverses a zero-crossing point of the magnetization M_Z at the position T_F^{BDPA} and T_F^{TEMPO}, respectively, indicated by arrows in Figure 2A,B. At this time value T_F, no Hahn echo is observed from this species by the detection sequence, and thus, this species is suppressed. We call this the filter time, T_F. If the different species have different recovery time traces, each species will have its own filter time T_F at which it is suppressed.

To obtain an IRf field-swept spectrum, the relaxation traces are recorded in a two-dimensional experiment where the magnetic field is swept in the second dimension. The suppression efficiency of the method for each individual compound is shown in the lower part of Figure 2A,B where field-swept spectra are recorded at the filter time of the pure compounds. For BDPA, this results in a 92% suppression at $T_F = 9$ μs, and for TEMPO, the suppression of the EPR signal is also 92% with a filter time of $T_F = 192$ ns.

In Figure 3A, the inversion-recovery spectrum of the TEMPO/BDPA mixture is shown. The field position where the spectrum is recorded is marked by an asterisk above the EPR spectrum shown in the insert. For comparison, the simulated inversion-recovery curves for the pure model compounds (using data listed in Table 1) are also shown (dashed lines). The relaxation curve of the mixture consists of a superposition of the relaxation curves of each individual component. When the detection sequence is applied at the two filter times, T_F^{BDPA} or T_F^{TEMPO}, indicated by the arrows in Figure 3A, it is possible to record a pure field-swept spectrum of the other compound. At the position T_F^{TEMPO}, the EPR signal consists only of the contribution from BDPA (Figure 3B), while at T_F^{BDPA}, the only contribution arises from TEMPO (Figure 3C). For the species with the longer relaxation time (BDPA), the signal observed is inverted and results in a signal intensity corresponding to 35% of the maximum intensity for BDPA. Because of the much shorter relaxation time of TEMPO almost 100% of the maximum signal intensity is detected. The individual spectra obtained from the mixtures are in very good agreement compared with the spectra of the pure components as can be seen from the difference spectra shown for each species at the bottom of Figure 3B,C.

Figure 4 shows a relaxation-filtered hyperfine (REFINE) experiment, which in this case uses a three-pulse ESEEM sequence, as shown in Figure 1B, applied to the model system CuHis-BDPA. The three-pulse ESEEM without the inversion-recovery filter performed at $g \approx 2$ is shown in Figure 4A. The time trace after echo decay subtraction reveals a superposition of slow and fast modulations. The slow modulation arises from nitrogen coupling of histidine to copper, while the fast modulation is assigned to protons of BDPA. After Fourier transformation, the respective proton (15 MHz) and nitrogen (0−3 MHz) frequencies are clearly

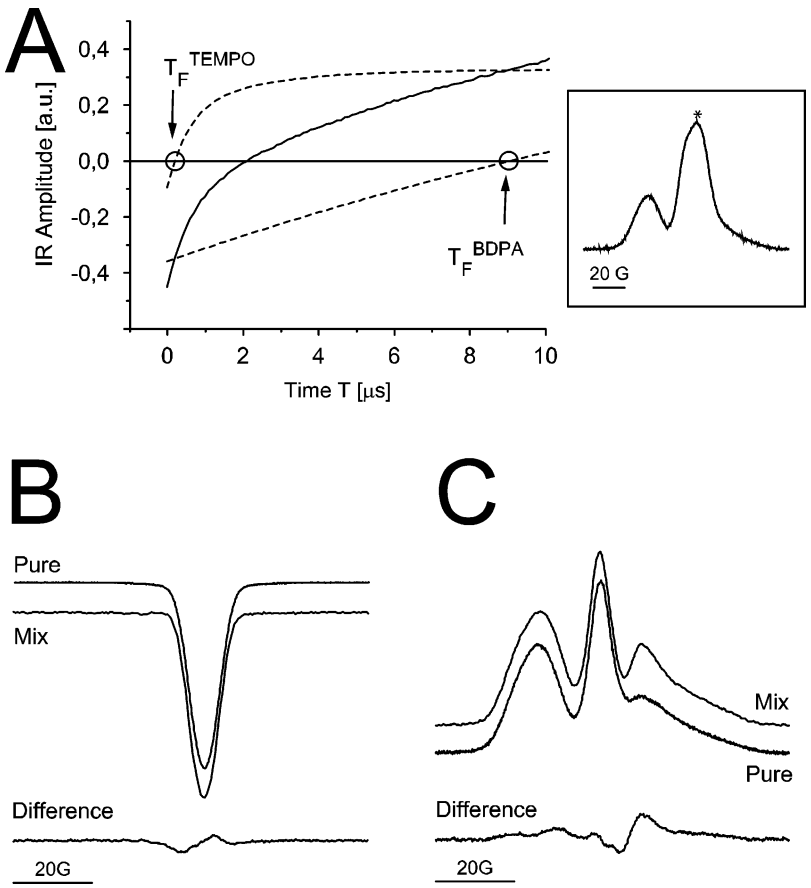

FIGURE 3: IRf field-swept spectra of the model compounds. Panel A depicts the inversion-recovery trace of a TEMPO/BDPA mixture. For comparison, the simulation of the inversion-recovery curves of the pure compounds are also drawn in the figure. Field position for the inversion-recovery trace is marked in the EPR spectrum (insert) by an asterisk. Panel B depicts the IRf field-swept spectrum at a filter time $T_F = 192$ ns. Comparison of the pure BDPA spectrum and the spectrum obtained from the mixture is shown. Panel C depicts the IRf field-swept spectrum at a filter time $T_F = 9$ μs. Comparison of the pure TEMPO spectrum and the spectrum obtained from the mixture is shown.

Table 1: Inversion-Recovery Parameters for TEMPO and BDPA[a]

	I^s [au]	T^s [μs]	I^f [au]	T^f [μs]	T_F^{calcd} [μs]
TEMPO	0.45	2.27	0.82	0.56	0.19
BDPA	0.92	42.00	0.44	17.00	9.07

[a] Fits were performed according to eq 1.

observed. With the application of the REFINE experiment (Figure 1B), it is possible to record the ESEEM spectrum of each individual compound from the mixture. At a filter time $T_F = 12.5$ μs, only the fast modulation of the protons from BDPA can be seen in the time trace and the respective Fourier transformed spectrum (Figure 4B). To selectively study the nitrogen modulations, a filter time $T_F = 1.5$ ms was chosen (Figure 4C). This filter time leads to a complete suppression of the modulations arising from the protons of BDPA, and only the nitrogen frequencies of the histidine are observed in the Fourier transformed spectrum.

2. Complex I. As mentioned previously, the detection of iron-sulfur clusters using cw-EPR is strongly dependent on temperature. At low temperatures, up to five iron-sulfur clusters of *Y. lipolytica* complex I are visible in the cw-EPR spectrum (*33*). At the specific temperature of 17 K, only the two iron-sulfur clusters, N1 and N2, contribute to the EPR spectrum in a pulsed experiment (Figure 5A). In a cw-EPR experiment, however, four iron-sulfur clusters are visible at this temperature. This difference can be explained by the fast relaxation times, T_2, of the iron-sulfur clusters. From cw spectra taken at 17 K a S/N ratio of 1200 can be determined compared to a S/N ratio of about 500 determined in the pulsed experiment (as defined in Materials and Methods).

The principal values of the **g**-tensor of the individual species are indicated in Figure 5. At the low field edge of the spectrum the g_z component of iron-sulfur cluster N2 is completely separated from any contribution from cluster N1. The g_z component of cluster N1 is also clearly visible while the two g_{xy} components overlap completely. Applying the IRf field-swept experiment as demonstrated for the model compounds, it is possible to separate the two FeS clusters (Figure 5B,C). Using a filter time $T_F^{N1} = 420$ ns, one can selectively record the spectrum of cluster N2 (Figure 5B). For cluster N1, this is possible with $T_F^{N2} = 68$ ns (Figure 5C). The EPR spectra so obtained can be simulated using the **g**-tensor values given in Table 2.

Figure 6 shows the REFINE sequence (Figure 1B) applied to the two iron-sulfur clusters N1 and N2 at a field value corresponding to $g = 1.96$. At this field position, both iron-sulfur clusters contribute equally to the intensity in the EPR spectrum. Filter times are selected to suppress the contributions of N1 and N2. Figure 6A shows an ESEEM trace with the respective Fourier transformation recorded with a filter time $T_F = 50$ μs. At this filter time, the system is back at the thermal equilibrium polarization. In the region of

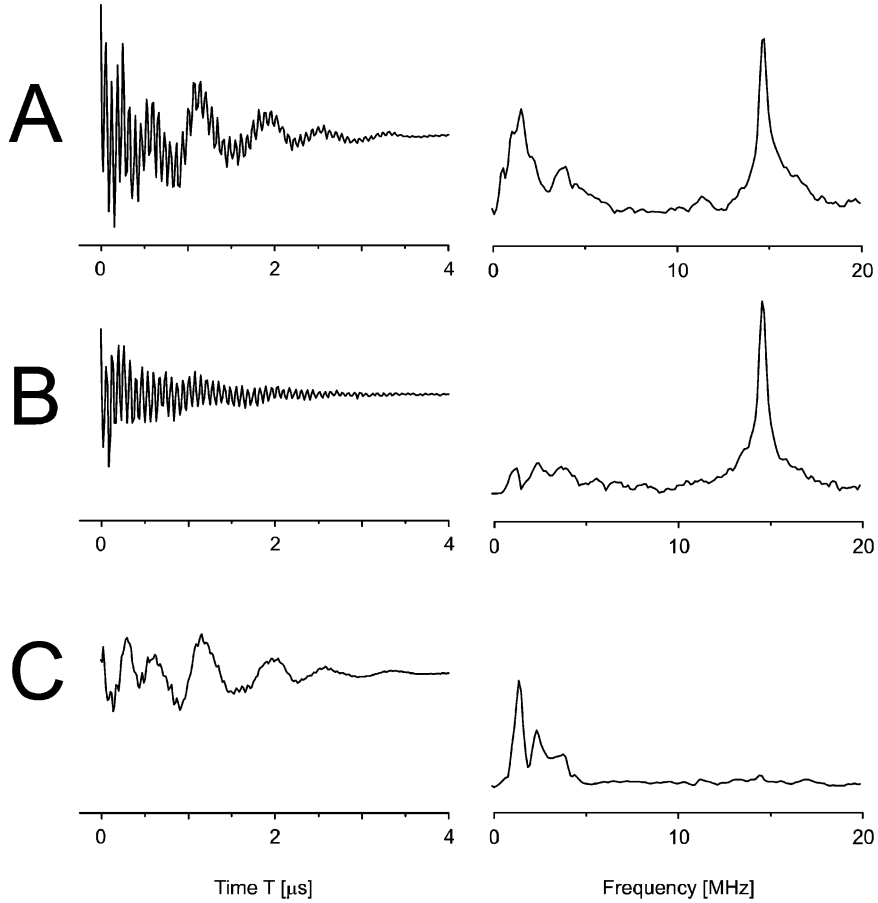

FIGURE 4: ESEEM and REFINE spectra of the model system CuHis-BDPA studied a 20 K. For all experiments, a τ value of 172 ns is used. All spectra are taken at $g \approx 2$. Panel A depicts the three-pulse ESEEM spectrum of CuHis−BDPA. Panel B depicts the REFINE spectrum at filter time $T_F = 12.5$ μs. Only contributions of BDPA are observed. Panel C depicts the REFINE spectrum with a filter time $T_F = 1.5$ ms. Only contributions of CuHis are observed.

0−4.5 MHz, several features are visible, which can be clearly assigned to a nitrogen nucleus, because of their Larmor frequency shift when changing the field position (data not shown). However, because of the overlap of the EPR spectra, it is not possible to decide which iron-sulfur cluster is responsible for these frequencies. By applying the filter sequence with the respective filter times T_F^{N1} and T_F^{N2}, one can record ESEEM spectra of the individual species. Figure 6B shows the ESEEM spectrum at a time where cluster N1 is completely suppressed. This time trace and the corresponding Fourier transformation do not show any modulations arising from the interaction with a nitrogen. Figure 6C shows the corresponding spectrum in which all contributions of cluster N2 are suppressed. The modulations that were observed in the REFINE spectrum with the 50 μs filter time are also observed in this spectrum.

DISCUSSION

1. Model Compounds. The inversion-recovery filter (IRf) presented here provides an experimental method for separating overlapping EPR signals in pulsed EPR experiments. Although, the relaxation mechanisms affecting the inversion-recovery experiment lead to a complex and often nonexponential decay as mentioned previously, this does not limit the application of the IR filter in practical cases. The feasibility and limitations of the presented IRf method are discussed in the following.

For the mixture of TEMPO and BDPA, only 8% of the original signal intensity is left at the observed filter times (Figure 2A,B, bottom). This residual signal appears as a perturbation in the signal of the mixture. However, this perturbation is scaled by the relative contributions of the two species in the mixture at the field position under study as well as the relative percentage of the observed signal at the separation time chosen. This is nicely demonstrated for BDPA in Figure 3B. The differences between the TEMPO spectrum recorded in the mixture and the pure compound itself arise mainly from anisotropic relaxation of T_1. For a successful separation of the individual components, it is clear that the relaxation behavior of each paramagnetic species should not have a large field dependence; otherwise, the two spectra cannot be separated with a fixed value of T_F. Such anisotropic relaxation of T_1 will affect different parts of the TEMPO spectrum differently. At the filter time of 9 μs, the central line of the TEMPO spectrum is nearly completely relaxed (99%), whereas the amplitude of the high-field line is still only at 94% of the total signal intensity. Thus when comparing the entire spectrum of TEMPO measured with IRf field-swept (at a time where the relaxation process is not complete) with a normal field-swept spectrum, small differences are expected and are seen (Figure 3B). However, the intensity of the calculated residual (which also includes the residual BDPA signal, Figure 2A) is still only ~20% of the total signal intensity.

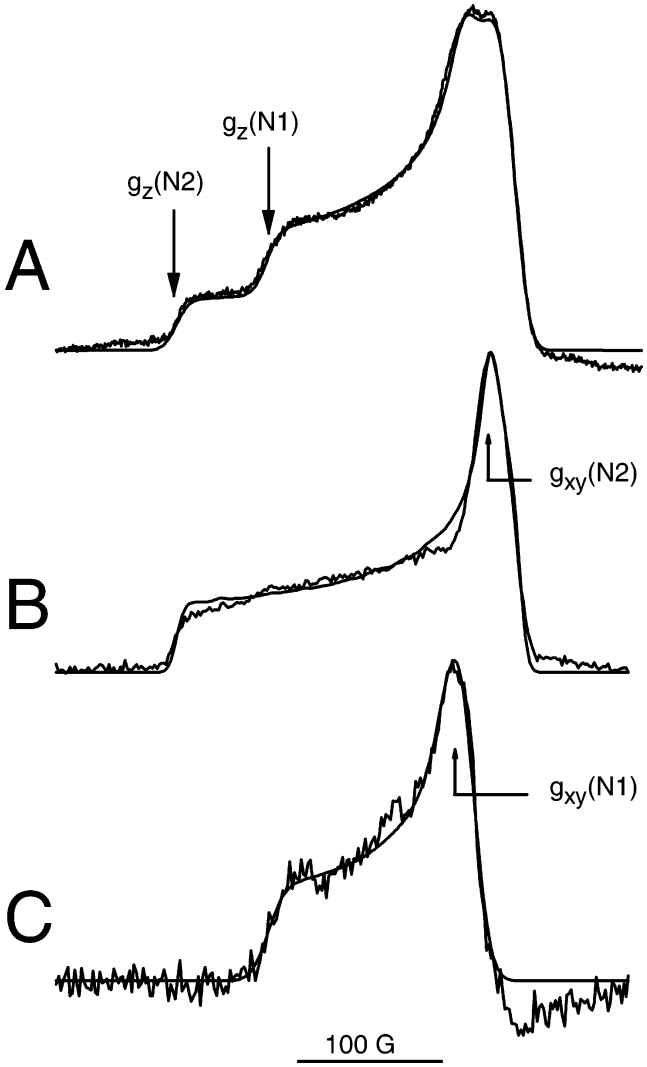

FIGURE 5: Field-swept EPR spectra of the iron-sulfur clusters of *Y. lipolytica* at 17 K with their respective simulations. Panel A presents the field-swept spectrum of *Y. lipolytica* at 17 K. The arrows indicate some principal values of the **g**-tensors of N1 and N2. Panel B presents cluster N2 with IRf field-swept spectrum at a filter time $T_F = 420$ ns. Panel C presents cluster N1 with IRf field-swept spectrum at a filter time $T_F = 68$ ns. The signal was multiplied by the factor of -1. Simulation parameters are given in Table 2. Within the estimated error of $\Delta g = 0.003$, it is possible to simulate all three spectra with the same values. The ratio of N1/N2 was calculated to be 55:45.

Table 2: Experimentally Determined *g*-Values for the FeS Clusters N1 and N2 from Different Organisms

cluster	organism	g_z	g_y	g_x
N1	*N. crassa*[a]	2.019	1.935	1.933
	bovine heart[b]	2.02	1.94	1.92
	Y. lipolytica[c]	2.020	1.943	1.940
	Y. lipolytica (IRf-FS)[d]	2.016	1.943	1.936
N2	*N. crassa*[a]	2.051	1.925	1.926
	bovine heart[b]	2.05	1.92	1.92
	Y. lipolytica[c]	2.053	1.929	1.925
	Y. lipolytica (IRf-FS)[d]	2.053	1.930	1.920

[a] *Neurospora crassa*; taken from ref *42*. [b] Taken from ref *8*. [c] Taken from ref *33*. [d] This work, simulated using a Gaussian line width of 13 G (N1) and 6 G (N2).

If the relaxation parameters of a mixture of two spins are both isotropic, it is possible to calculate the filter times by a simple method. When an unknown system is studied, one important requirement is that at least one field position in the EPR spectrum belongs to only one species. At this position, it is straightforward to record an inversion-recovery trace to determine the relaxation parameters for the first species. The parameters for the second species can be extracted from an inversion-recovery trace recorded at a position where both species contribute to the signal. The time trace recorded at this position is fitted by a multiexponential function, whereby only the parameters of the second species are varied. The relaxation parameters determined from the inversion-recovery curves for the TEMPO/BDPA mixture using eq 1 are summarized in Table 1. After the time traces of each individual species with their respective parameters are simulated and the traces are plotted in a semilogarithmic representation, the decay function crosses a horizontal line corresponding to the echo intensity without inversion (data not shown). The time at this point corresponds to the respective filter time (T_F) of each individual component. These mathematically determined filter times are given in Table 1 and are in excellent agreement with the experimentally determined values of 192 ns for TEMPO and 9 μs for BDPA.

In addition, we have used these numerical simulations to estimate the range of conditions required for a successful REFINE (IRf) experiment on such a mixture of two compounds. The ratio of the respective T_1 ratios is varied from 1:2 to 1:10 while changing the degree of inversion and the S/N level. For a given S/N of 500 in a pulsed experiment, the limit for the ratio T_1^A/T_1^B is estimated to be 1:5. The ideal ratio of signal amplitudes (I^A/I^B) is 1:1 but may vary by one order of magnitude under the conditions defined above. In principle, there is no minimum filter time T_F using a phase cycling sequence, however, without a phase cycling sequence the minimum filter time has to be in the order of $2\tau \approx 500$ ns.

The requirements for a successful experiment are summarized as follows: (1) T_1 of each species has to be isotropic; (2) S/N $\geq$ 1000 in a cw-experiment; (3) $T_F > 500$ ns (without phase cycling); (4) $T_1^A/T_1^B \geq 1/5$ (for a given S/N of 500 in a pulsed experiment); (5) $I^A/I^B \geq 0.1$ for detection of A and suppression of B (for a given S/N of 500 in a pulsed experiment)

The feasibility of REFINE is clearly demonstrated on the model system CuHis-BDPA (Figure 4). From IRf field-swept experiments, the suppression of the CuHis contribution was estimated to be at least 85% of the total signal intensity of CuHis at $g \approx 2$. For BDPA, the suppression is 90%. As can be clearly seen from Figure 4, even with an incomplete suppression, the different hyperfine contributions are still sufficiently separated.

This method opens up several other possibilities. The REFINE concept can be extended into a second dimension with one dimension corresponding to the filter time T_F and the other to the time domain of the ESEEM experiment. Thus even without knowing the filter times of two paramagnetic species, it should still be possible to assign different ESEEM transitions to different species by the time-dependent response of the individual hyperfine lines. This should then also be possible when more than two species contribute to the ESEEM spectra and the relaxation times cannot be measured directly via inversion recovery.

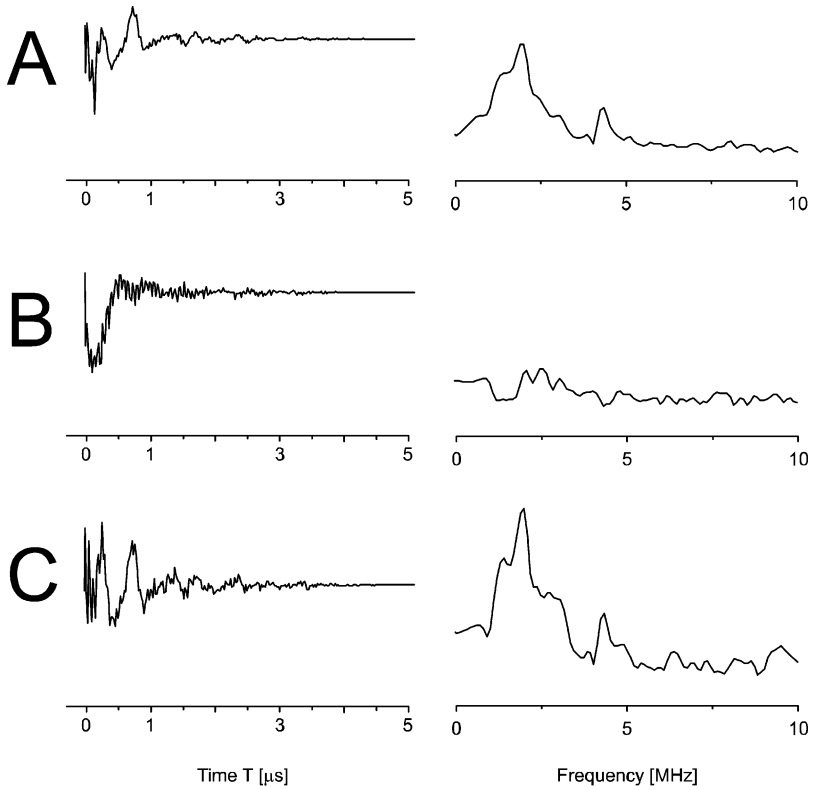

FIGURE 6: REFINE spectra of complex I at 17 K. For all experiments, a τ value of 192 ns is used. All spectra are taken at a magnetic field corresponding to $g = 1.96$ and are normalized to the echo intensity at $t = 0$. Panel A presents the REFINE spectrum with a 50 μs filter time. Panel B presents the REFINE spectrum with a filter time to suppress the contributions of cluster N1. No modulations are left. Panel C presents the REFINE with a filter time taken to suppress contributions of cluster N2.

2. Complex I. The relaxation behavior of iron-sulfur clusters has been extensively studied using cw-EPR saturation methods (*35*). In the temperature range of 5−30 K, the spin-lattice relaxation usually occurs via a Raman process, as has been shown for [2Fe−2S] clusters (*36*), as well as for [4Fe−4S] clusters (*37*), and the Debye temperature for both types of FeS clusters is in the range of 60 K (45 cm^{-1}).

The IRf field-swept experiment is successfully applied to the two FeS clusters N1 and N2 of complex I of *Y. lipolytica*. In principle, it should be possible to predict the filter time for each FeS cluster by calculation as shown for the model system TEMPO/BDPA. This requires that the correct values for the relaxation parameters can be extracted from the inversion-recovery traces. Unfortunately in biological systems, it is often the case that additional minority paramagnetic species of variable intensity contribute to the EPR spectrum, making this simple analysis of such inversion-recovery traces very difficult. In the case of complex I, it is not possible to calculate an exact value for the filter times. Instead a two-dimensional experiment has to be performed to determine the filter times (T_F^{N1} and T_F^{N2}) where the first dimension corresponds to the field-swept EPR spectrum and the second dimension to the filter time T_F. The filter times of $T_F^{N1} = 420$ ns and $T_F^{N2} = 68$ ns determined by this experiment were then applied to suppress the contribution of one or the other iron-sulfur cluster in the EPR spectrum. The signal intensities using the inversion-recovery filter are 28% for cluster N1 and 58% for cluster N2 compared to the intensities without use of the filter. Despite these reduced signal intensities, an adequate S/N is still achievable within reasonable measuring times.

The *g*-values for the iron-sulfur clusters N1 and N2 determined from simulation of the IRf field-swept spectrum are compared with values obtained by cw-EPR for different organisms (Table 2). The IRf field-swept spectra can each be satisfactorily fitted with only one **g**-tensor (Table 2), demonstrating that the obtained separation times lead to a good suppression of the other species within the experimental S/N ratio and are in very good agreement with the values taken from the literature. Within the estimated error of $\Delta g = 0.003$, it is possible to simulate the EPR spectrum of the mixture as well as those of the individual species with the same *g*-values (Figure 5). In addition, the ratio of N1/N2 is determined to be 55:45. This result confirms our previous determination of the stoichiometry of iron-sulfur clusters in complex I from *Y. lipolytica*, which was 1:1:1:1 for the clusters N1, N2, N3, and N4 (*31*). The complex I samples do not show any unassigned spectroscopic contributions that might indicate the presence of an additional binuclear cluster like N1a in the bovine or *E. coli* enzyme. On the other hand, the binding motif for a second 2Fe−2S cluster is conserved in the corresponding *Y. lipolytica* subunit. Possibly this cluster is not sufficiently reduced because of an extremely negative redox midpoint potential.

Because no crystal structure of complex I is available, it is of great interest to study the immediate ligand sphere of cluster N2 with alternative spectroscopic methods. At a temperature of 30 K where only cluster N1 is visible, we have also observed spin-echo modulations that can be assigned to nitrogen. Thus with conventional ESEEM spectroscopy alone, it will not be easy to distinguish between possible modulations arising from either N1 or N2 at 17 K.

However, using REFINE, it is possible to study the hyperfine spectrum of cluster N2 alone. From Figure 6B, it is shown that the modulations observed in the ESEEM spectrum at 17 K can be clearly assigned to cluster N1 and are very similar to those seen at 30 K for N1 alone (data not shown).

Two different types of cluster coordination are typical for [2Fe−2S] clusters, namely, a Rieske- and a ferredoxin-type, having characteristic patterns in their ESEEM spectrum. While the Rieske ESEEM spectrum is dominated by two double quantum peaks around 4 and 7 MHz (e.g., see refs *20*, *38*, and *39*), the ESEEM spectra of ferredoxins only reveal several peaks below 5 MHz (e.g., see refs *21*, *22*, *40*, and *41*). This difference is because the magnitude of the hyperfine tensor for a backbone nitrogen in ferredoxins ($\bar{A} \approx 1$ MHz) is closer to the exact cancellation condition ($2\nu_I = A$) compared to the hyperfine tensor value of the remote histidine in Rieske centers ($\bar{A} \approx 4$ MHz). These characteristics provide a fingerprint that can be used to describe the ESEEM spectrum of cluster N1. Assuming that cluster N1 corresponds to cluster N1b known from bovine and bacterial complex I, this cluster is not expected to have a direct nitrogen ligand but rather is coordinated by four cysteines. This fact and the fingerprint obtained for cluster N1 indicates a ferredoxin-type [2Fe−2S] cluster interacting with a peptide backbone nitrogen.

When the contribution of cluster N1 is completely suppressed, no nitrogen modulations are observed in the REFINE spectrum of cluster N2. From the fact that cluster N2 does not show any ^{14}N ESEEM effect, we can most probably exclude a direct coordination by a histidine or another amino acid having nitrogen in the side chain.

CONCLUSIONS

It has been shown that an inversion-recovery filter can be used to separate the spectral contributions from different paramagnetic species in a pulsed EPR experiment. This was first demonstrated for the model compounds BDPA and TEMPO in polystyrene. The application of this inversion-recovery filter together with hyperfine spectroscopy (REFINE) was shown for the three-pulse ESEEM sequence to selectively suppress contributions of a mixture of two species in the ESEEM experiment. This novel method was then applied to complex I from *Y. lipolytica*. It was possible to record individual EPR spectra of iron-sulfur clusters N1 and N2 within one sample at the same temperature. This cannot be achieved by conventional cw- or pulsed EPR methods. The obtained signal intensities are sufficient to obtain EPR spectra of the individual components within acceptable measurement times. Finally it could be shown with REFINE spectroscopy that cluster N2 is most probably not coordinated by a nitrogen from an amino acid side chain. This REFINE concept should be applicable for all types of hyperfine spectroscopic methods (e.g., HYSCORE, ENDOR, TRIPLE) allowing the detailed investigation of overlapping EPR signals separately. In addition, this inversion-recovery filter may also be combined with other pulse sequences such as PELDOR. Such REFINE experiments are currently being performed in our laboratory.

REFERENCES

1. Beinert, H. (2000) Iron-sulfur proteins: ancient structures, still full of surprises, *J. Biol. Inorg. Chem. 5*, 2−15.
2. Membrane proteins of known structure, Max Planck Institute for Biophysics, (2003) http://www.mpibp-frankfurt.mpg.de/michel/public/memprotstruct.html.
3. Videira, A. (1998) Complex I from the fungus *Neurospora crassa*, *Biochim. Biophys. Acta 1364*, 89−100.
4. Brandt, U., Kerscher, S., Dröse, S., Zwicker, K., and Zickermann, V. (2003) Proton and sodium pumping by complex I (NADH: ubiquinone oxidoreductase) through redox driven conformational energy transfer? *FEBS Lett. 545*, 9−17.
5. Wikström, M. K. F. (1984) Two protons are pumped from the mitochondrial matrix per electron transfer between NADH and ubiquinone, *FEBS Lett. 169*, 300−304.
6. Weiss, H., and Friedrich, T. (1991) Redox-linked proton translocation by NADH-ubiquinone reductase (complex I), *Biochim. Biophys. Acta 23*, 743−771.
7. Shapira, A. H. (1998) Human Complex I defects in neurodegenerative diseases, *Biochim. Biophys. Acta 1364*, 261−270.
8. Ohnishi, T. (1998) Iron−sulfur clusters/semiquinones in Complex I, *Biochim. Biophys. Acta 1364*, 186−206.
9. Yano, T., and Ohnishi, T. (2001) The origin of cluster N2 of the energy-transducing NADH-quinone oxidoreductase: comparisons of phylogenetically related enzymes, *J. Bioenerg. Biomembr. 33*, 213−222.
10. van Belzen, R., Kotlyar, A. B., Moon, N., Dunham, W. R., and Albracht, S. P. J. (1997) The iron-sulfur clusters 2 and ubisemiquinone radicals of NADH:Ubiquinone oxidoreductase are involved in energy coupling in submitochondrial particles, *Biochemistry 36*, 886−893.
11. Ingledew, W., and Ohnishi, T. (1980) An analysis of some thermodynamic properties of iron-sulphur centers in site I of mitochondria, *J. Biochem. 186*, 111−117.
12. Magnitsky, S. (2002) EPR characterization of ubisemiquinones and iron-sulfur cluster N2, central components of the energy coupling in the NADH-ubiquinone oxidoreductase (Complex I) in situ, *J. Bioenerg. Biomembr. 34*, 193−208.
13. Brandt, U. (1997) Proton-translocation by membrane-bound NADH:ubiquinone-oxidorecuctase (complex I) through redox-gated ligand conduction, *Biochim. Biophys. Acta 1318*, 79−81.
14. Brandt, U. (1999) Proton translocation in the repiratory chain involving ubiquinone − a hypothetical semiquinone switch mechanism for complex I, *BioFactors 9*, 95−101.
15. Friedrich, T., Brors, B., Hellwig, P., Kintscher, L., Rasmussen, T., Scheide, D., Schulte, U., Mäntele, W., and Weiss, H. (2000) Characterization of two novel redox groups in the respiratory NADH:ubiquinone oxidoreductase (complex I), *Biochim. Biophys. Acta 1459*, 305−309.
16. Duarte, M., Populo, H., Videira, A., Friedrich, T., and Schulte, U. (2002) Disruption of iron-sulphur cluster N2 from NADH: ubiquinone oxidoreductase by site-directed mutagenesis, *J. Biochem. 364*, 833−839.
17. Kerscher, S., Dröse, S., Zwicker, K., Zickermann, V., and Brandt, U. (2002) *Yarrowia lipolytica*, a yeast genetic system to study mitochondrial complex I, *Biochim. Biophys. Acta 1555*, 83−91.
18. Kashani-Poor, N., Zwicker, K., Kerscher, S., and Brandt, U. (2001) A central functional role for the 49-kDa subunit within the catalytic core of mitochondrial complex I, *J. Biol. Chem. 276*, 24082−24087.
19. Garofano, A., Zwicker, K., Kerscher, S., Okun, P., and Brandt, U. (2003) Two Aspartic Acid Residues in the PSST-Homologous NUKM Subunit of Complex I from *Yarrowia lipolytica* are Essential for Catalytic Activity, *J. Biol. Chem. 278*, 42435−42440.
20. Britt, R. D., Sauer, K., Klein, M. P., Knaff, D. B., Kriauciunas, A., Yu, C.-A., Yu, L., and Malkin, R. (1991) Electron Spin-Echo Envelope Modulation Spectroscopy Supports the Suggested Coordination of Two Hisitidine Ligands to the Rieske Fe-S Centers of the Cytochrome b_6f Complex of Spinach and the Cytochrome bc_1 Complexes of *Rhodospirillum rubrum*, *Rhodobacter sphaeroides* R-26, and Bovine Heart Mitochondria, *Biochemistry 30*, 1892−1901.
21. Dikanov, S. A., Tyryshkin, A. M., Felli, I., Reijerse, E. J., and Hüttermann, J. (1995) C-Band ESEEM of Strongly Coupled Peptide Nitrogens in Reduced Two-Iron Ferredoxin, *J. Magn. Reson. 108*, 99−102.
22. Cammack, R., Chapman, A., McCracken, J., Cornelius, J. B., Peisach, J., and Weiner, J. H. (1988) Electron spin-echo spectroscopic studies of *Escherichia coli* fumarate reductase, *Biochim. Biophys. Acta 956*, 307−312.
23. Prisner, T. F. (1997) Pulsed high-frequency/high-field EPR, *Adv. Magn. Opt. Res. 20*, 245−299.

24. Eichel, R.-A., and Schweiger, A. (2001) Electron-Zeeman resolved electron paramagnetic resonance spectroscopy, *J. Magn. Reson. 152*, 276−287.
25. Stoll, S., Jeschke, G., Willer, M., and Schweiger, A. (1998) Nutation-Frequency correlated EPR spectroscopy: The PEANUT experiment, *J. Magn. Reson. 130*, 86−96.
26. Hofbauer, W., and Bittl, R. (2000) A novel approach to separating EPR lines arising from species with different transition moments, *J. Magn. Reson. 147*, 226−231.
27. Lawrence, C. C., Bennati, M., Obias, H. V., Bar, G., and Griffin, R. G. (1999) High-field EPR detection of a disulfide radical anion in the reduction of cytidine 5′-diphosphate by the E441Q R1 mutant of *Escherichia coli* ribonucleotide reductase, *Proc. Natl. Acad. Sci U.S.A. 96*, 8979−8984.
28. Yoshida, H., and Ichikawa, T. (1993) Electron Spin-Echo Studies of Free Radicals in Irradiated Polymers, *Adv. Polym. Sci. 105*, 3−36.
29. Hoffmann, E., and Schweiger, A. (1995) Inversion-recovery detected EPR, *Appl. Magn. Reson. 9*, 1−22.
30. Mims, W. B. (1972) Envelope modulation in spin-echo experiments, *Phys. Rev. B 5*, 2409−2419.
31. Dröse, S., Zwicker, K., and Brandt, U. (2002) Full recovery of the NADH:ubiquinone activity of complex I (NADH:ubiquinone oxidoreductase) from *Yarrowia lipolytica* by the addition of phospholipids, *Biochim. Biophys. Acta 1556*, 65−72.
32. Kashani-Poor, N., Kerscher, S., Zickermann, V., and Brandt, U. (2001) Efficient large scale purification of his-tagged proton translocating NADH:ubiquinone oxidoreductase (complex I) from the strictly aerobic yeast *Yarrowia lipolytica*, *Biochim. Biophys. Acta 1504*, 363−370.
33. Djafarzadeh, R., Kerscher, S., Zwicker, K., Rademacher, M., Lindahl, M., Schägger, H., and Brandt, U. (2000) Biophysical and structural characterization of proton-translocating NADH-dehydrogenase (complex I) from the strictly aerobic yeast *Yarrowia lipolytica*, *Biochim. Biophys. Acta 1459*, 230−238.
34. Gemperle, C., Aebli, G., Schweiger, A., and Ernst, R. R. (1990) Phase cycling in pulse EPR, *J. Magn. Reson. 88*, 241−256.
35. Eaton, S. S., and Eaton, G. R. (2000) in *Biological Magnetic Resonance* (Eaton, G. R., Ed.) pp 29−154, Kluwer Academic/Plenum Publishers, New York.
36. Gayda, J.-P., Bertrand, P., Deville, A., More, C., Roger, G., Gibson, J. F., and Cammack, R. (1979) Temperature dependence of the electronic spin-lattice relaxation time in a 2-iron-2-sulfur protein, *Biochim. Biophys. Acta 581*, 15−26.
37. Bertrand, P., Gayda, J.-P., and Rao, K. K. (1982) Electron spin-lattice relaxation of the (4Fe-4S) ferredoxin from *B. stearothermophilus*. Comparison with other iron proteins, *J. Chem. Phys. 76*, 4715−4719.
38. Shergill, J. K., and Cammack, R. (1994) ESEEM and ENDOR studies of the Rieske iron-sulphur protein in bovine heart mitochondrial membranes, *Biochim. Biophys. Acta 1185*, 35−42.
39. Shergill, J. K., Joannou, C. L., Mason, J. R., and Cammack, R. (1995) Coordination of the Rieske-Type [2Fe-2S] Cluster of the Terminal Iron-Sulfur Protein of *Pseudomonas putida* Benzene 1,2-Dioxygenase, Studied by One- and Two-Dimensional Electron Spin-Echo Envelope Modulation Spectroscopy, *Biochemistry 34*, 16533−16542.
40. Riedel, A., Fetzner, S., Rampp, M., Lingens, F., Liebl, U., Zimmermann, J.-L., and Nitschke, W. (1995) EPR, Electron Spin-Echo Envelope Modulation, and Electron Nuclear Double Resonance Studies of the 2Fe-2S Centers of the 2-Halobenzoate 1,2-Dioxygenase from *Burkholderia (Pseudomonas) cepacia* 2CBS, *J. Biol. Chem. 270*, 30869−30873.
41. Shergill, J. K., Golinelli, M.-P., Cammack, R., and Meyer, J. (1996) Coordination of the [2Fe-2S] Cluster in Wild-Type and Molecular Variants of *Clostridium pasterurianum* Ferredoxin, Investigated by ESEEM Spectroscopy, *Biochemistry 35*, 12842−12848.
42. Wang, D.-C., Meinhardt, S. W., Sackmann, H., Weiss, H., and Ohnishi, T. (1991) The iron-sulfur clusters in the two related forms of mitochondrial NADH: ubiquinone oxidoreductase made by *Neurospora crassa*, *Eur. J. Biochem. 197*, 257−264.

BI035865E